

Equation of state data for gold in the pressure range <10 TPa

Dimitri Batani,* Antonio Balducci, Daniele Beretta, and Andrea Bernardinello

Dipartimento di Fisica "G. Occhialini", Università degli Studi di Milano-Bicocca, and INFN, Via Emanueli 15, 20126 Milano, Italy

Thorsten Löwer

Max Planck Institut für Quantenoptik, D-85740 Garching, Germany

Michel Koenig, Alessandra Benuzzi, and Bernard Faral

Laboratoire pour l'Utilisation des Lasers Intenses, Unité mixte UMR 7605, CNRS-CEA-Ecole Polytechnique-Université Pierre et Marie Curie, Ecole Polytechnique, 91128 Palaiseau, France

Tom Hall

Department of Physics, University of Essex, Wivenhoe Park, Colchester CO4 3SQ, Great Britain

(Received 15 June 1999; revised manuscript received 28 October 1999)

We report experimental data on the equation of state of gold in the pressure range 2–10 TPa obtained using laser-driven shock waves. The experiments have been realized using an iodine high-power laser with subnanosecond pulses and techniques like phase zone plates and hohlraums to produce spatially uniform shocks. Our data are compared with existing equation of state models.

I. INTRODUCTION

The study of equations of state (EOS) of matter in high-pressure conditions (above 1 TPa or 10 Mbar) is a subject of great interest for several fields of modern physics. In particular, it is important in the context of astrophysics, material science, and inertial confinement fusion research. Some EOS already exist for this pressure range,¹ but, first, they mainly come from calculations and theoretical models, with only a few experimental data available to validate them, and furthermore they exist for a restricted number of materials. Therefore the behavior of many materials under high pressure is still unknown. In the past, EOS measurements in the TPa range could be performed only by nuclear explosions. Nowadays, it is possible to reach very high pressures in the laboratory by using powerful pulsed laser-generated shock waves in solid materials. Earlier experiments have shown the possibility of producing shock waves with pressures up to 10 TPa in a laser-irradiated solid^{2,3} and in a target foil impacted by a laser accelerated foil.⁴ Pressures as high as 75 TPa were achieved by using laser pulses of 25 kJ (at wavelength $\lambda = 0.53 \mu\text{m}$) and a foil impact technique.⁵ In another experiment, 2-TPa planar shocks were produced by employing 2.2-kJ laser pulses.⁶ However, in many of these experiments the bad quality of shocks prevented them from being used as a quantitative tool in high-pressure physics.

Planarity of the shock fronts and low preheating in the material ahead of the shock waves are essential to obtain accurate measurements of EOS. Recent experiments^{6,7} have proved the possibility of creating spatially very uniform shocks in solids by using two different methods. The first one consists in producing shock waves by direct heating of the target with the laser (direct drive) with optically smoothed laser beams; the second method uses the laser irradiation converted into x-ray thermal radiation to generate shocks (indirect laser drive).

Although difficult, the control of preheating has been assured in both methods. In the indirect drive method, the experiments by Löwer *et al.*⁶ have clearly shown that preheating is very sensitive to the geometry of the cavity. Special cavities⁸ have been designed to minimize the preheating of the target, produced by direct primary x-rays, to a negligible value.⁹

In direct drive, the control of preheating has been achieved through the combined use of several experimental means: the use of optical smoothing techniques to avoid high-intensity laser hot spots, irradiation with shorter-wavelength laser light as compared to the infrared fundamental frequency, and the use of low-Z ablaters. These reduce x-ray emission from the laser-ablated material and hence preheating effects ahead of the shock wave. (At the same time such techniques were applied, diagnostic methods had to be developed in order to measure the preheating temperature of the target.^{10–12})

Only if high-quality shocks are obtained, it is possible to perform precise measurements of the shock parameters. In particular, EOS points can be obtained if two quantities of the shocked material, related to the Hugoniot-Rankine relations,¹³ are measured simultaneously. In a recent important experiment conducted with the Nova laser at the Livermore Laboratory,¹⁴ this method has been applied to measure the EOS of deuterium at pressures as high as 0.3 TPa. The main problem connected with such a method is that it is applicable only to low-Z materials, which are transparent to x rays, and that it is necessary to use high-energy laser pulses with the aim of maintaining a constant ablation pressure for a few nanoseconds and of irradiating large target areas.

Another method for the determination of EOS points has been optimized,^{15,16} actually before the one used at Livermore, and already used to get EOS data for Cu,¹⁷ foams,¹⁸ and doped plastic.¹⁹ It is based on the impedance-matching technique and consists in measuring the shock velocity si-

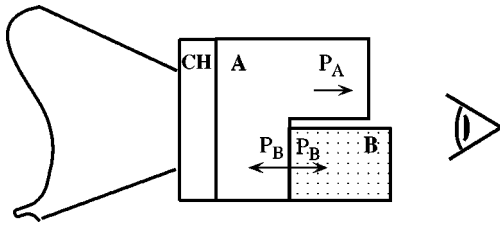


FIG. 1. Double step targets with a common base and two steps of different materials, A and B. From the shock traveling time in these steps, measured with a visible streak camera, the shock velocities D_A and D_B are determined. P_A and P_B are the corresponding pressures.

multaneously (on the same laser shot) in two different materials (see Fig. 1). This makes it possible to achieve a relative determination of an EOS point of one material by taking the EOS of the other one as a reference. This is a classical method for EOS determination (see, for instance, Ref. 13 on calibrated reflection), already used in nuclear-driven experiments²⁰ and proposed many years ago for laser experiments.²¹ Anyway, it could never be exploited before the work in Ref. 15 for laser experiments in the TPa range due to poor shock quality.

The target is made of a “base” foil made of a material A, which is irradiated by the laser on one side and supports, on the opposite side, two steps made, respectively, of the same material A and of a different material B (the CH ablator layer in Fig. 1 may or may not be present to reduce x-rays). Using rear-face, time-resolved imaging, we experimentally determine the velocity of the shock propagating through the two steps D_A and D_B (corresponding to particle velocities U_A and U_B , respectively). If the EOS (and hence also the Hugoniot curve) of the base material is known, we can determine an EOS point for material B. This is a “relative” measurement since it uses material A as a reference. In order to find the EOS point for B, we consider the intersection in the (P, U) plane of the line $P = \rho_B D_B U$, where ρ_B is the density of cold B material, with the reflected shock polar drawn from the point (P_A, U_A) . The line $P = \rho D U$ is one of the Hugoniot-Rankine equations¹³ and represents momentum conservation across the shock front. The direct and reflected shock polar for material A give the relation between the fluid velocity U and shock pressure P in the shocked material and are derived from the EOS of A which is known. The method is illustrated in Fig. 2.

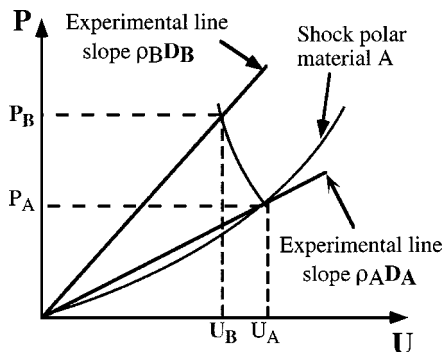


FIG. 2. Calibrated reflection method, used to determine EOS points for gold (material B)

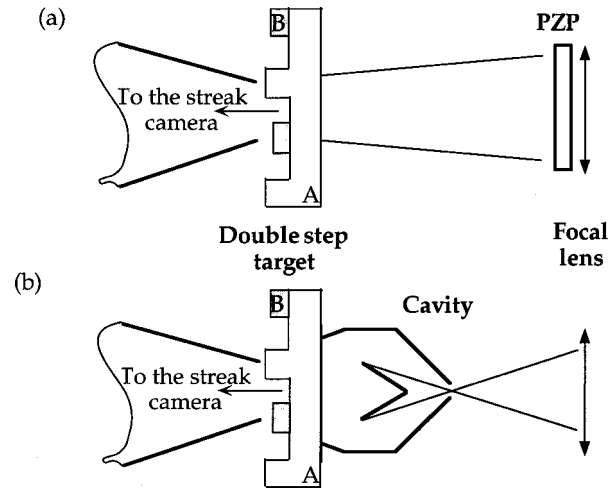


FIG. 3. Experimental setup at MPQ. PZPs and cavities are used for production of high-quality shocks.

In this paper we report the application of such a technique to measure the EOS of gold at pressure $P > 2$ TPa (actually up to 10 TPa), using laser irradiation, and two-step, two-material targets. Gold EOS data are crucial, since this is an important material for radiation confinement studies in astrophysics and Inertial Confinement Fusion, being used for hohlraum production and because it is a typical reference high-Z material.^{22,23} The experiments have been realized using an iodine high-power laser with subnanosecond pulses and phase zone plates to produce spatial smoothing of the beams. Our data are represented on shock polars (plots of shock pressure P vs fluid velocity U) and velocity plots (plots of shock velocity D vs fluid velocity U), two common ways of presenting EOS data obtained from shock experiments. Also, our data are compared with existing shock polars and velocity plots obtained from different equations of state models. Excluding the few data obtained for a few materials with nuclear explosions, these are the EOS points at the highest pressure available up to now.

With respect to previous similar experiments,¹⁵ here we not only reached much higher pressures, but also realized a better control of shock planarity and target preheating, as discussed in the paper, allowing a higher degree of confidence in obtained experimental results.

II. EXPERIMENTAL SETUP

The experiment was performed using the Asterix iodine laser of the Max Planck Institut für Quantenoptik, which delivers a single beam, 30 cm in diameter, with an energy of 250 J per pulse at a wavelength of $0.44 \mu\text{m}$. The temporal behavior of the laser pulse is Gaussian with a full width at half maximum (FWHM) of 450 ps. In order to generate the shock wave into the target, we used direct and indirect laser drive. Figure 3 shows the two different schematic experimental setups.

In the direct laser drive configuration [Fig. 3(a)] the laser beam was focused directly onto the target with a $f = 564$ mm lens ($f/2$ aperture). The primary condition of producing high-quality flat shock fronts imposed the use of the phase zone plate (PZP) (Ref. 24) optical beam smoothing technique, in order to eliminate the large-scale spatial inten-

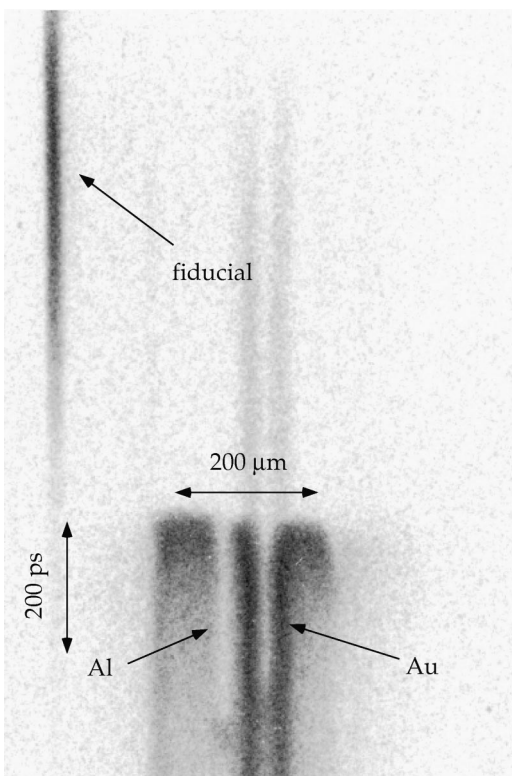


FIG. 4. Image of shock breakout obtained at MPQ with indirect drive.

sity modulations arising from the coherent nature of the laser light and to produce a flat-top intensity distribution in the focal spot. The design of this plate had Fresnel lenses of 2.5 cm diameter, which implies that 144 Fresnel lenses are covered by the laser beam. The characteristics of our optical system (PZP+focusing lens) were such that we produced a total focal spot of $400\ \mu\text{m}$ FWHM, with a $250\text{-}\mu\text{m}$ wide flat region in the center, corresponding to a laser intensity $I_L \leq 4 \times 10^{14}\ \text{W}/\text{cm}^2$.

In the indirect laser drive configuration [Fig. 3(b)], we focused the laser beam into a millimeter-size gold cavity through a small entrance hole (with the same focusing lens used in the direct laser drive configuration). An isotropic thermal radiation is then created²² whose temperature depends on the cavity size and the laser power. It can be determined by observing the velocity of a shock wave generated when radiation is absorbed in low- Z material.²² In our experiment it has been measured to be in the range of 100–150 eV. Our cavity (called Labyrinth cavity⁸) has been designed not only to achieve such high temperatures, but also to optimize the irradiation uniformity when only one laser beam is used and to minimize the preheating of the target, produced by direct primary x rays. Here a shield with a conical shape has been constructed so that the laser irradiated area and the shocked material were not in direct view of each other, as shown in Fig. 3(b). Measurements, made in silicon with shock pressures in the 0.4–0.8 TPa range, had shown that the increase in temperature due to preheating is not higher than 150–200 K.⁹

While it was well known that the indirect drive could ensure a very high degree of planarity,⁸ the main advantage of direct drive is its intrinsic high efficiency, allowing much

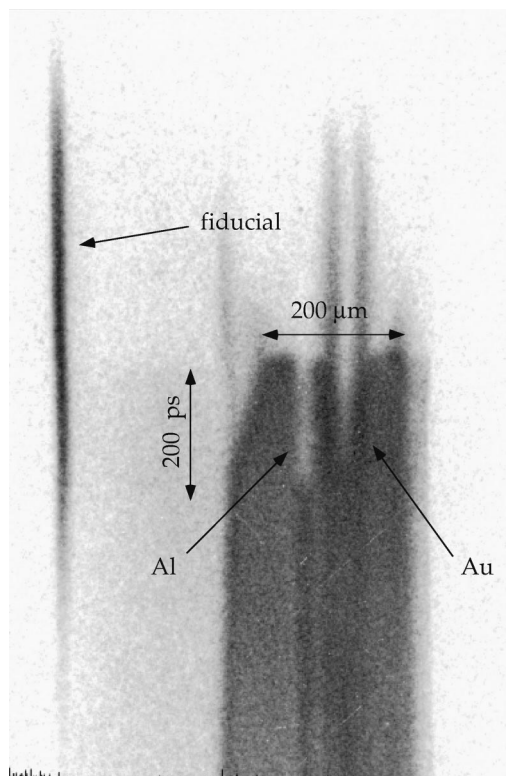


FIG. 5. Image of shock breakout obtained at MPQ with PZP and Al/Au targets.

higher pressures to be reached with the same laser energy.¹⁷

The diagnostic used to detect the shock emergence from the target rear face consisted of an $f/2$ objective, with a focal length $f=100\ \text{mm}$, imaging the rear face onto the slit of a streak camera, working in the visible region. The temporal resolution was better than 8 ps and the imaging system magnification was $M=10$, allowing a spatial resolution better than $10\ \mu\text{m}$. A protection system⁸ was also used for the diagnostic light path, to shield the streak camera from scattered laser light.

The targets were composed of aluminum (reference material) and gold (“unknown” material) and have been made at the Laboratoire des Cibles of the Commissariat à l’Energie Atomique at Limeil-Valenton. Large samples ($2\ \text{cm} \times 2\ \text{cm}$) were produced from which individual targets were then cut. The accurate fabrication technique²⁵ allowed sharp step edges to be obtained and a precise determination of step heights. The Al base thickness was of $10.25\ \mu\text{m}$, while the steps’ thicknesses were $5.5\text{--}6.4\ \mu\text{m}$ for Al and $2.4\text{--}3.03\ \mu\text{m}$ for Au. A few targets had a $18\text{-}\mu\text{m}$ Al base.

Three different experimental setups were realized at MPQ: (1) indirect drive+Al/Au targets, (2) direct drive+PZP+Al/Au targets, and (3) direct drive+PZP+CH/Al/Au targets

Figures 4–6 show streak camera images of shock breakouts obtained in each case. The case (3), Fig. 6, was realized in order to focus the laser on a low- Z material (CH), producing low x-ray emission; this was done to avoid any possible preheat which could have been present in case (2), Fig. 5 (also the impedance mismatch between CH and Al was useful in order to increase the pressure in Al). The typical plastic thickness was $5\ \mu\text{m}$. We see the time fiducial obtained by

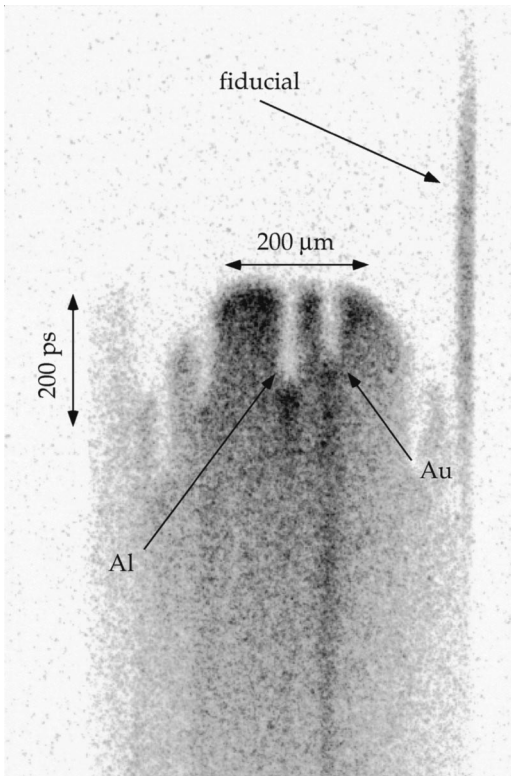


FIG. 6. Image of shock breakout obtained at MPQ with PZP and CH/Al/Au targets.

sending a portion of the laser beam on the streak camera slit through a fiber.

III. DISCUSSION OF EXPERIMENTAL ERRORS

EOS experiments aim at discriminating between different theoretical models, when these are available, or at acquiring completely new data in unexplored pressure regimes in order to drive the development of EOS models. In most cases the pressure deviations between the models do not exceed 10%,^{1,23,26,27} which sets an upper limit of about 5% to the experimental accuracy required in the measurement of the shock velocity. Of course, even less precise data may be very useful if they fall in previously unexplored regions.

In our case there are three main sources of possible errors in the determination of D : the quality of the shock itself (requiring flatness over a wide region), the sweep speed (ps/mm) of the streak camera, and knowledge of the step thicknesses and roughness.

In our experiment the shock emergence from the target was inferred by detection of the emission of the target rear face in the visible region. This was imaged by a photographic objective onto the slit of a visible streak camera with 8 ps time resolution. Also, the sweep of our streak camera was affected by a relative error lower than 1%, as verified by calibrating the streak camera with an étalon made of a series of short laser pulses produced by multiple reflection between two glass layers at a known distance.²⁸ The step heights and surface roughness were measured with a profilometer (Dek-Tak) and resulted in being better than $0.03 \mu\text{m}$. Since the thicknesses of the aluminum and gold steps were about 6 and $2.5 \mu\text{m}$, respectively, this ensured a relative error in thick-

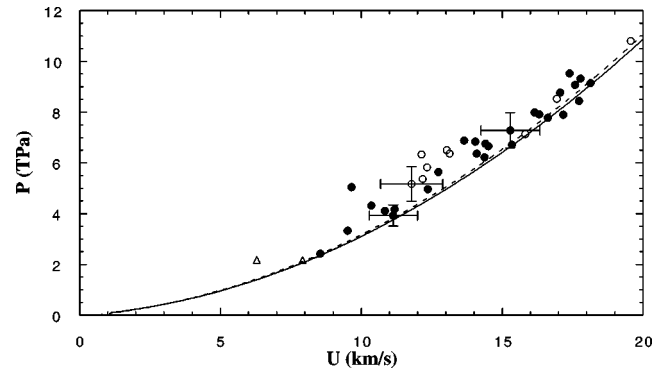


FIG. 7. Experimental data and comparison with the Sesame (solid curve) and MPQEOS (dashed curve) shock polars. Triangles, indirect drive+Al/Au targets; open circles, direct drive+PZP+Al/Au targets; solid circles, direct drive+PZP+CH/Al/Au targets.

ness of about 0.5% for the aluminum step and about 1.2% for the gold step. Sample initial densities were determined using a microbalance to weigh the whole samples after deposition and profilometer to measure them.

Finally we checked the quality of the generated shock wave and found typical variations of ± 5 ps for the shock breakthrough time across the 200- μm flat region of the focal spot. With all the above errors taken into account and using a simple error propagation evaluation, the shock velocities were determined with a maximum error of $\pm 7.5\%$ in aluminum and $\pm 10\%$ in gold (this not only includes the instrumental errors, but also the errors made in reading experimental data).

In deducing the error in the Au pressure and fluid velocity, it is possible to show explicitly that they are about the same. Moreover, we found that the relative error in the shock pressure is approximately twice as that in the shock velocity, in accordance with the approximate quadratic dependence¹³ between the two quantities.

IV. EXPERIMENTAL RESULTS

The obtained data are shown in Fig. 7 in the (P,U) plane and are compared with the shock polar obtained from the Sesame EOS and the Max Planck Institut für Quantenoptik EOS (MPQEOS).²⁷ We considered also a different model, The Temperature EOS (TEOS),²⁶ but since it is very close to MPQEOS, it has not been represented in Fig. 7.

When we take into account the experimental errors in fluid velocity and shock pressure (of the order of a few percent; see Sec. V for a detailed discussion), most of the points (but not all of them) are really consistent with Sesame. However, the trend of our experimental data is clearly showing that, for a given fluid velocity, the experimental pressure is higher than Sesame. So either Sesame is not correct in the range $4 \leq P \leq 10$ TPa, or there is a systematic error in our data which could be due to nonstationarity or to the presence of preheating ahead of the shock wave, problems which will be discussed in the next section, while we will discuss in Sec. VI the implications of our experimental data.

We also note that, although the Al equation of state is well known, different models can anyway be used producing slightly different results. If an alternative Al EOS is used,

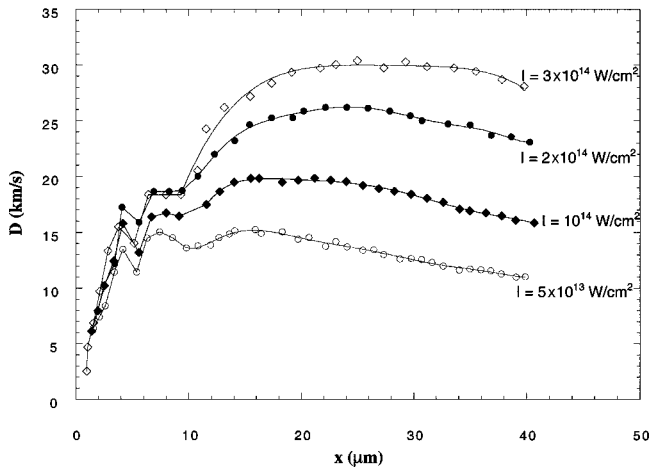


FIG. 8. Numerical simulation of shock velocity vs position of the shock in a CH/Al target: CH thickness is $5 \mu\text{m}$. Simulations were made for four laser intensities: $I_L = 3 \times 10^{14} \text{ W/cm}^2$ (open diamonds); $I_L = 2 \times 10^{14} \text{ W/cm}^2$ (solid circles); $I_L = 1 \times 10^{14} \text{ W/cm}^2$ (solid diamonds); $I_L = 5 \times 10^{13} \text{ W/cm}^2$ (open circles).

then the results for gold will be slightly different. The use of the TEOS gives a slightly bigger fluid velocity U for the same measured shock velocity D . However, the general trend of our experimental data remains the same.²⁹

V. DISCUSSION OF PREHEATING AND SHOCK STATIONARITY

A first reason which could explain the departure of our experimental data from existing EOS models could be the shock quality; i.e., either the shock is nonstationary under the given experimental conditions or there is preheating. The question of planarity is solved by the use of beam smoothing and the use of sufficiently thin targets. Furthermore, we checked it on each laser shot thanks to the high spatial resolution of the diagnostics. Hence we now address the two other points.

Nonstationarity of the shock front can be due at early times to the shock arrival at the target base before it has reached its maximum pressure and a constant velocity. At later times the shock wave may decay either due to bidimensional expansion effects or to the fact that, after the end of the laser pulse, the relaxation wave originating from the target front side reaches the shock front before it emerges from either the Al or the Au step. Two-dimensional (2D) effects are in our case negligible thanks to the use of the beam smoothing techniques and the fact that the typical thickness of the used targets (at most $22 \mu\text{m}$) is definitely smaller than the central flat region of the focal spot ($250 \mu\text{m}$).

Hence, in order to check that the shock pressure is constant inside each step, we performed hydrodynamic 1D simulations, with the code MULTI.³⁰ These showed that in our irradiation conditions ($I < 4 \times 10^{14} \text{ W/cm}^2$) the base must be thicker than approximately $9 \mu\text{m}$ to reach stationarity. From Fig. 8 we observe that using CH/Al/Au targets we obtain quite stationary shocks (better than with simpler Al/Au targets). Indeed Fig. 8 shows that for thickness between 15 and $21 \mu\text{m}$ (the step interval) the maximum variation in shock velocity is smaller than 5% for $I \approx 2 \times 10^{14} \text{ W/cm}^2$, which

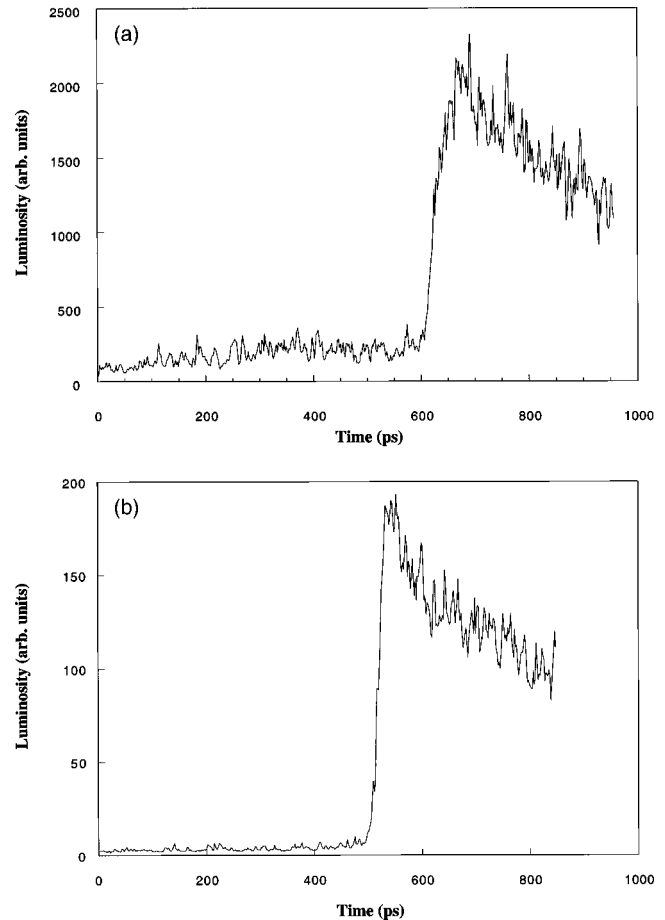


FIG. 9. Time-resolved luminosity of the shock-heated aluminum target. (a) Signal obtained with direct drive. Shock pressure $\approx 20 \text{ Mbar}$, target thickness = $15.75 \mu\text{m}$. (b) Signal obtained with indirect drive. Shock pressure $\approx 9 \text{ Mbar}$, target thickness = $16.48 \mu\text{m}$.

corresponds to most of our shots (for some shots intensity was about 10^{14} W/cm^2 , corresponding to a maximum variation in shock velocity smaller than 1%). Since this variation is the difference between the maximum and minimum shock velocity in the step, it implies a variation in the shock breakout time which is less than 5%. Even for other laser intensities, the induced variations in shock breakout time are less than the sources of errors previously analyzed.

Another, experimental, proof of shock stationarity arises from the pictures in Figs. 4–6, which show a comparable luminosity for shock breakout at the Al base and Al step. Indeed, luminosity is also dependent on shock pressure and is more sensitive than shock velocity to small variations in shock pressure, as shown in Ref. 8.

The main question that pushed us to use CH/Al/Au targets [case (3)] is that of preheating. Even if during this experiment we did not take any particular effort to measure preheating directly, we think that our measurements are *not* affected by any strong preheating for the following reasons.

(a) The temporal shape of the rear side luminescence, as can be seen in Fig. 9, is consistent with the absence of significant preheating; i.e., it is characterized by a fast decay time and an even faster rise time (the connection between target preheating and backside emission has been studied

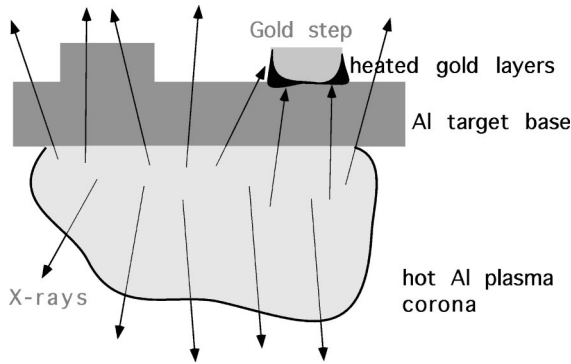


FIG. 10. Mechanism of luminescence at the edges of the gold step due to Al x rays emitted from the plasma corona.

experimentally in Refs. 6, 10 and 11 and numerically in Refs. 11 and 31).

(b) Preheating would produce an early luminosity, but this would originate uniformly from the step rear side, and not be concentrated on the step edges, as instead we can observe in Fig. 5.

(c) The data obtained in cases (3) and (1) do not show any really significant difference from the data obtained in case (2). If there was preheating, this would have been strongly reduced by adding about $5\ \mu\text{m}$ of plastic as in case (3).

(d) Data obtained for Cu with the same experimental setup and laser intensities fit quite well with the Cu Sesame tables.¹⁷ Preheating is determined by the material of the target base and by absorption in the steps. Here the base was Al, as in Ref. 17, which means that x-ray production was the same in the two cases. Moreover, the step is made in Au which absorbs x rays more strongly than Cu. This means that x rays are absorbed in a layer closer to the base-step interface, which is thinner in the case of Au as compared to the case of Cu. Hence the motion of the shock wave, around the time of shock breakout, should be less influenced than in the case of the Cu EOS experiment.

Excluding preheating, the question arises of the cause of the early luminosity seen in images obtained in case 2 (Fig. 5), at the edges of the gold step. We think that the explanation is as follows.

(i) A hot Al plasma corona is created from the Al base which emits x rays mainly in lines below the Al K edge ($\approx 1.6\ \text{keV}$).

(ii) The Al base and step are rather transparent to such radiation and hence they only slightly absorb it, producing a negligible heating and emission from Al step.

(iii) On the contrary, gold is very opaque to such radiation and absorbs it in a very thin layer at the edges and around the interface. The edges are then heated to a temperature sufficient to produce significant visible emission (see Fig. 10).

Hence we think that the luminosity which is present in type-(2) targets is not due to preheating (in the usual meaning of the word). Anyway, the presence of such early emission luminescence made it difficult to measure the breakout time precisely. This was the cause of a larger error as compared to type-(3) targets. In particular the reading error is increased of a factor which has been evaluated, on many shots, to be of the order of 2, and this explains why type-(2) targets are characterized by larger experimental errors in Fig. 7.

VI. DISCUSSION

The gold EOS has been studied in the past using light-gas guns,^{32,33} chemical explosives,^{34–36} and collisions with an impactor.^{33,35–37} The old works by McQueen and co-workers^{34,37} are included in the Los Alamos Laboratory data,³³ and the more recent work by Al'tshuler *et al.*³⁶ includes the older data from the same group.³⁵ The data obtained were limited to $P < 0.58\ \text{TPa}$ and showed that the relation between D and U was practically linear, $D = C + SU$, where $C \approx 3.12\ \text{km/s}$ is of the order of the sound velocity in the material [which is $3.24\ \text{km/s}$ Ref. 38] and $S \approx 1.5$. We note that the line $D = C + SU$ corresponds in the (P, u) plane to a parabola going through the origin, i.e., of the form $P = aU + bU^2$, which is physically meaningful since it implies $U = 0$ at $P = 0$.

Unlike other materials, gold was not studied using nuclear explosions (these data have been published in some recent reviews³⁹) or at least such data are not available. Hence until a few years ago no measurements on the Au Hugoniot were available at pressures higher than $0.58\ \text{TPa}$. A recent experiment with laser-driven shock waves¹⁵ has measured the gold equation of state up to pressures $\leq 3.5\ \text{TPa}$. In this pressure range (and at higher pressures, up to $10\ \text{TPa}$) there is a small, but significant difference between Sesame and other models such as MPQEOS and TEOS.

The TEOS model^{26,29} has been developed on the basis of available information up to $0.58\ \text{TPa}$. It yields values which are practically identical to the MPQEOS model²⁷ developed following the same physical principles of the ‘‘Quotidian’’ EOS model (QEOS).⁴⁰ However, the accuracy of the data in Ref. 15 and the fact that higher pressures were not reached in the experiment did not allow discriminations between such models.

Such higher pressures have been reached in the present experiment. The accuracy in shock velocity in our experiment, as explained in Sec. III, is not too high ($\approx 7.5\%$ in Al, $\approx 10\%$ in Au) as compared to that obtained in experiments reported in the literature at lower pressures. However, the accuracy in the parameters of the Hugoniot is better than 10% since they are determined by fitting a $D = C + SU$ line with a high number of experimental points.

Also, we have averaged the different experimental results obtained for the same shock velocity D (the experimentally measured parameter) to get the data presented in Fig. 11. By this method, already used in others works, e.g., in Ref. 36, it is possible to reduce experimental errors down to $4\%–8\%$ for shock velocity. Moreover, in Fig. 11 we have considered only shots obtained with a plastic layer. Even if all data show the same trends, those with plastic gave the best camera images and hence correspond to the smallest reading errors. Figure 11 also shows the experimental data obtained at $P \leq 0.6\ \text{TPa}$ from conventional experiments^{32–37} and at pressures $1–3.5\ \text{TPa}$ by Koenig *et al.*¹⁵

As expected, Fig. 11 confirms the already observed systematic deviation of our experimental points from Sesame (Fig. 7). MPQEOS and TEOS lay above Sesame, and so the agreement with such models is slightly better. However, even such models do not seem to describe the behavior of our data completely. In order to understand the origin of such a deviation, excluding systematic errors in our experiments

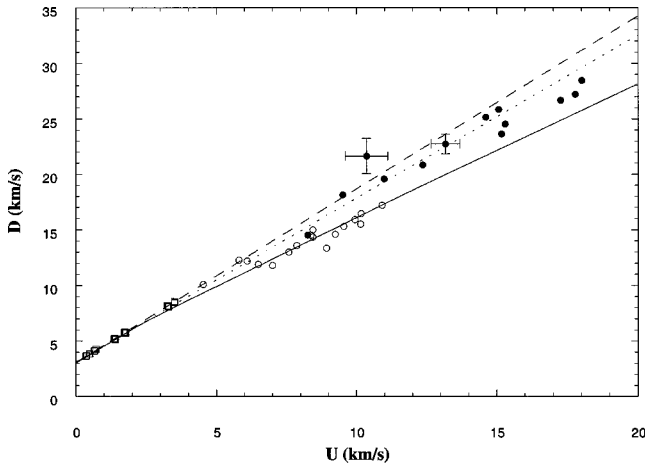


FIG. 11. Experimental data in the D vs U plane. Present experiment (solid circles), LULI experimental data (open circles) from Ref. 15 and experimental points at lower pressures from Refs. 32 and 34–37 (open squares) are compared with Sesame (solid curve), McQueen and Marsh (Ref. 37) (dashed curve) and Al'tshuler *et al.* (Ref. 35) (dotted curve) fitting equations.

(Sec. IV), we considered the extrapolations to high pressures of the fits to experimental data at lower pressures from Refs. 35 and 37. The agreement with our data is much better, as shown in Fig. 11. This suggests that interpolations from Refs. 35 and 37 describe correctly gold also above the pressure range for which they have been obtained.

Finally, we have compared Sesame to the experimental points presented in Refs. 32, 34, 35 and 37.

As we can see in Fig. 12, around a pressure of 0.6 TPa Sesame already disagrees significantly from experimental data (in particular from those by Jones *et al.*³²). Our data, and the fits from experimental data obtained in previous years, seem to suggest that gold is less compressible than what predicted by many theoretical models at pressures lower than 1 TPa. The disagreement between Sesame and

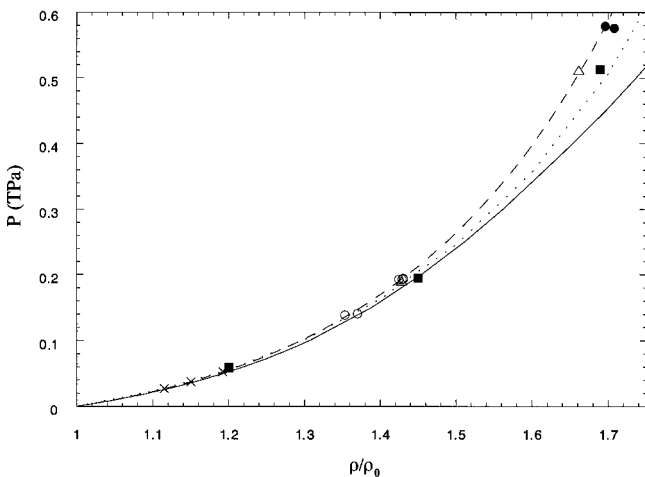


FIG. 12. Experimental points obtained by Walsh *et al.* (Ref. 34) (crosses), Al'tshuler *et al.* (Ref. 35) (squares), Al'tshuler *et al.* (Ref. 36) (triangles), McQueen and Marsh (Ref. 37) (open circles), Jones *et al.* (Ref. 32) (solid circles) compared on the plane P vs ρ/ρ_0 with Sesame curve and the Al'tshuler *et al.* (Ref. 35) (dotted curve) and McQueen and Marsh (Ref. 37) (dashed curve) fitting equations.

experimental data at pressures ≥ 0.6 TPa deserves some more comments.

A change in the slope of the curve obtained from the Sesame tables is evident in the graph of Fig. 11 for $D \approx 7$ km/s. Below this value, Sesame agrees with the fitting curves to experimental data obtained with conventional methods. Actually, the Hugoniot fit used in the Sesame tables is $D = 3.12 + 1.521U$,⁴¹ which is quite close to that reported in Refs. 35–37. At high pressures Au Sesame is built with the Barnes-Cowan-Rood method,^{42,43} using data reported in Refs. 44–46. The intersection between the two curves produces a slope change which corresponds to a phase transition. Although the transition region may not be correctly described by such simple superposition of the two models, it is evident that such phase transition does not seem to be present in the experimental results. This could mean that Sesame does not correctly describe the behavior of gold at high pressures (starting already at $P \approx 0.6$ TPa).

An alternative explanation is that the short time scale used in our experiment does not allow such phase transition to be observed. Indeed, the actual time needed by a shock compressed material to reach thermodynamic equilibrium is not precisely known and it is the object of current research which must be performed using diagnostics with a much higher temporal resolution, in order to study the detailed temporal structure of the shock wave.⁴⁷

Finally, the difference between our data and Sesame (or other EOS) could be explained by some other mechanism inducing a systematic deviation of our data, which we have not been able to discover, or have underestimated, in the present paper.

VII. CONCLUSIONS

In conclusion, the reported experiment has shown the possibility of obtaining quantitative measurements on shock waves in a solid sample directly irradiated by optically smoothed laser beams. The pressure regime $P \leq 10$ TPa was explored by employing a laser system with a pulse energy of ≈ 250 J per shot. The use of PZP allowed the production of high-quality, flat shock fronts.

The method has been applied to obtain EOS data for gold in the pressure range 2–10 TPa. These are the experimental points at the highest pressure obtained up to now with laser-driven shock waves. Such data seem to show a compressibility for gold significantly lower than that predicted by the Sesame tables. In particular, at $P \approx 10$ TPa gold compressibility is $\rho/\rho_0 \approx 3.4$ following the Sesame tables, and only $\rho/\rho_0 \approx 2.6$ extrapolating the fits by Al'tshuler *et al.*³⁵ If confirmed by other measurements and theories, this may have important consequences, e.g., for the design of ICF hohlraums and in general for all the fields of physics where the behavior of high-pressure material is important.

ACKNOWLEDGMENTS

This work has been supported by the European Program “TMR: Access to Large Scale Facilities” and realized at the Max Planck Institut für Quantenoptik, in Garching. We warmly acknowledge the technical support of the MPQ staff. We also thank Simone Bossi, Flavia Torsiello, Arianna Mo-

relli, and Laura Müller, University of Milano-Bicocca, for their help. We thank Professor Igor Krasnyuk, Dr. Victor Mintsev, and Dr. Igor Lomonosov of the Russian Academy of Science for the very useful discussions, for their suggestions and for the availability of the TEOS model. Such contributions have taken place in the framework of the INTAS-

RFBR program on “Laser driven Shock waves.” Finally we thank J. Meyer-ter-Vehn and A. Kemp, MPQ Garching, M. Lontano, CNR (Consiglio Nazionale delle Ricerche), Milano, and E. Tosatti and C. Cavazzoni, SISSA (Scuola Internazionale Superiore di Studi Avanzati), Trieste, for the useful discussions and comments.

*Electronic address: batani@mi.infn.it

- ¹SESAME Report on the Los Alamos Equation-of-State library, Report No. LALP-83-4 (T4 Group LANL, Los Alamos, 1983).
- ²C. G. M. van Kessel and R. Sigel, *Phys. Rev. Lett.* **33**, 1020 (1974); L. R. Veeder and S. C. Solem, *ibid.* **40**, 1391 (1978); R. J. Trainor, J. W. Shaner, J. M. Auerbach, and N. C. Holmes, *ibid.* **42**, 1154 (1978); F. Cottet *et al.*, *ibid.* **52**, 1884 (1984); J. D. Kilkenny, University of California Report No. UCRL 50021-86, 1987 (unpublished), pp. 3–6.
- ³F. Cottet *et al.*, *Appl. Phys. Lett.* **47**, 678 (1985).
- ⁴R. Fabbro *et al.*, *Laser Part. Beams* **4**, 413 (1986); S. P. Obenschain *et al.*, *Phys. Rev. Lett.* **50**, 44 (1983); B. Faral *et al.*, *Phys. Fluids B* **2**, 371 (1990).
- ⁵R. Cauble *et al.*, *Phys. Rev. Lett.* **70**, 2102 (1993).
- ⁶Th. Löwer, R. Sigel, K. Eidmann, I. B. Foldes, S. Hüller *et al.*, *Phys. Rev. Lett.* **72**, 3186 (1994).
- ⁷M. Koenig, B. Faral, J. M. Boudenne, D. Batani, S. Bossi, and A. Benuzzi, *Phys. Rev. E* **50**, R3314 (1994).
- ⁸Th. Löwer and R. Sigel, *Contrib. Plasma Phys.* **33**, 355 (1993); Th. Löwer and R. Sigel, in *High Pressure Science and Technology* (AIP, New York, 1996), p. 1261.
- ⁹Th. Löwer, V. N. Kondrashov, M. Basko, A. Kendl, J. Meyer-ter-Vehn, and R. Sigel, *Phys. Rev. Lett.* **80**, 4000 (1998).
- ¹⁰T. Hall, A. Benuzzi, D. Batani, D. Beretta, S. Bossi, B. Faral, M. Koenig, J. Krishnan, M. Mahdich, and Th. Löwer, *Phys. Rev. E* **55**, R6356 (1997).
- ¹¹A. Benuzzi, M. Koenig, B. Faral, J. Krishnan, F. Pisani, D. Batani, S. Bossi, D. Beretta, T. Hall, S. Ellwi, S. Hüller, J. Honrubia, and N. Grandjean, *Phys. Plasmas* **5**, 2410 (1998).
- ¹²J. Honrubia, R. Dezulian, D. Batani, S. Bossi, M. Koenig, A. Benuzzi, and N. Grandjean, *Laser Part. Beams* **16**, 1 (1998).
- ¹³Ya. B. Zeldovich and Yu. P. Raizer, *Physics of Shock Waves and High Temperature Hydrodynamic Phenomena* (Academic, New York, 1967).
- ¹⁴G. W. Collins, L. B. Da Silva, P. Celliers *et al.*, *Science* **281**, 1178 (1998).
- ¹⁵M. Koenig, B. Faral, J. M. Boudenne, D. Batani, S. Bossi, A. Benuzzi, C. Remond, J. Perrine, M. Temporal, and S. Atzeni, *Phys. Rev. Lett.* **74**, 2260 (1995).
- ¹⁶D. Batani, M. Koenig, Th. Löwer, A. Benuzzi, and S. Bossi, *Europhys. News* **27**, 210 (1996); D. Batani, S. Bossi, A. Benuzzi, M. Koenig, B. Faral, J. M. Boudenne, N. Grandjean, M. Temporal, and S. Atzeni, *Laser Part. Beams* **14**, 211 (1995).
- ¹⁷A. Benuzzi, Th. Löwer, M. Koenig, B. Faral, D. Batani, D. Beretta, C. Danson, and D. Pepler, *Phys. Rev. E* **54**, 2162 (1996).
- ¹⁸M. Koenig, A. Benuzzi, B. Faral, J. Krishnan, J. M. Boudenne, T. Jalinaud, C. Rémond, A. Decoster, D. Batani, D. Beretta, and T. A. Hall, *Appl. Phys. Lett.* **72**, 1033 (1998).
- ¹⁹M. Koenig, A. Benuzzi, B. Faral, D. Batani, L. Müller, F. Torsiello, T. Hall, N. Grandjean, and W. Nazarov (unpublished).
- ²⁰C. Ragan III, *Phys. Rev. A* **29**, 1391 (1984).
- ²¹N. C. Holmes, R. J. Trainor, and R. A. Anderson, in *Shock Waves in Condensed Matter*, edited by W. J. Nellis, L. Seaman, and R. A. Graham, AIP Conf. Proc. No. **78** (AIP, New York, 1982), p. 160.
- ²²J. Lindl, *Phys. Plasmas* **2**, 3933 (1995).
- ²³S. B. Kormer and V. D. Urlin, *Dokl. Acad. Nauk (SSSR)* **131**, 542 (1960) [*Sov. Phys. Dokl.* **5**, 317 (1960)].
- ²⁴R. M. Stevenson, M. J. Norman, C. Danson, I. Ross *et al.*, *Opt. Lett.* **19**, 363 (1994).
- ²⁵B. Faral *et al.*, *Rapport Scientifique LULI 1993*, 309 (1994) (unpublished).
- ²⁶A. Bushman, G. Konel, A. Ni, and V. Fortov, *Intense Dynamic Loading of Matter* (Taylor & Francis, London, 1993).
- ²⁷A. J. Kemp and J. Meyer-ter-Vehn, *Nucl. Instrum. Methods Phys. Res. A* **415**, 674 (1998).
- ²⁸Th. Löwer (private communication).
- ²⁹I. Lomonosov, I. Krasnyuk, and V. Mintsev (private communication).
- ³⁰R. Ramis, R. Schmalz, and J. Meyer-ter-Vehn, *Comput. Phys. Commun.* **49**, 475 (1988).
- ³¹D. Batani, A. Benuzzi, I. Krasnyuk, P. Pashinin, A. Semenov, I. Lomonosov, and V. Fortov, *Plasma Phys. Controlled Fusion* **41**, 93 (1999).
- ³²A. H. Jones, W. H. Isbell, and C. J. Maiden, *J. Appl. Phys.* **37**, 3493 (1966).
- ³³*LASL Shock Hugoniot Data*, edited by S. P. Marsh (University of California Press, Berkeley, 1980).
- ³⁴J. M. Walsh, M. H. Rice, R. G. McQueen, and F. L. Yarger, *Phys. Rev.* **108**, 169 (1957).
- ³⁵L. V. Al'tshuler, K. K. Krupnikov, and M. I. Brazhnik, *Zh. Eksp. Teor. Fiz.* **34**, 886 (1958) [*Sov. Phys. JETP* **7**, 614 (1958)].
- ³⁶L. V. Al'tshuler, A. A. Bakanova, I. P. Dudoladov, E. A. Dynin, R. F. Trunin, and B. S. Chekin, *Zh. Prikl. Mekh. Tekhn. Fiz.* **2**, 3 (1981) [*J. Appl. Mech. Tech. Phys.* **22**, 145 (1981)].
- ³⁷R. G. McQueen and S. P. Marsh, *J. Appl. Phys.* **31**, 1253 (1960).
- ³⁸*Handbook of Chemistry and Physics*, 63rd ed., edited by R. C. Weast (CRC Press, Cleveland, OH, 1983).
- ³⁹R. F. Trunin, *Phys. Usp.* **37**, 1123 (1994).
- ⁴⁰R. F. More, in *Laser Interaction and Related Plasma Phenomena*, edited by H. J. Schwarz *et al.* (Plenum, New York, 1981), Vol. 5, p. 253.
- ⁴¹M. van Thiel, Lawrence Livermore Laboratory Report No. UCRL-50108, Rev. 1, 1977 (unpublished).
- ⁴²R. D. Cowan and J. Ashkin, *Phys. Rev.* **105**, 144 (1957); J. D. Barnes, *Phys. Rev.* **153**, 269 (1967).
- ⁴³The equation of state in astrophysics, I A.U. Colloquium 147, edited by Chabrer, Gilles and Schatzman, Evry QB466.E65 (1994).
- ⁴⁴*Handbook of Chemistry and Physics*, edited by R. C. Weast (CRC Press, Cleveland, OH, 1976).
- ⁴⁵K. A. Gechnieder, Jr., *Solid State Phys.* **16**, 275 (1964).
- ⁴⁶L. Brewer, Lawrence Berkeley Laboratory Report No. LBL 3720, 1975 (unpublished).
- ⁴⁷A. Benuzzi, M. Koenig, J. M. Boudenne, T. Hall, F. Scianitti, A. Masini, and D. Batani, *Phys. Rev. E* **60**, R2488 (1999).